Running Title: Influence of the bone environment in osteosarcoma.

Bone environment is essential for osteosarcoma development from transformed mesenchymal stem cells

Ruth Rubio[1*], Ander Abarrategi[2*], Javier Garcia-Castro[2*], Lucia Martinez-Cruzado[3], Carlos Suarez[3], Juan Tornin[3], Laura Santos[3], Aurora Astudillo[3], Isabel Colmenero[4], Francisca Mulero[5], Michael Rosu-Myles[6] Pablo Menendez[1,7,8§] and Rene Rodriguez[1,3§]

[1]GENyO. Centre for Genomics and Oncological Research: Pfizer / University of Granada / Andalusian Government, Granada, Spain. [2]Unidad de Biotecnología Celular, Área Biología Celular y del Desarrollo, Instituto de Salud Carlos III, Majadahonda, Madrid, Spain. [3]Hospital Universitario Central de Asturias and Instituto Universitario de Oncología del Principado de Asturias, Oviedo, Spain. [4]Servicio de Anatomía Patológica, Hospital Universitario Niño Jesús, Madrid, Spain. [5]Spanish National Cancer Reseach Center (CNIO), Molecular Imaging Core Unit, Madrid, Spain. [6]Health Canada Centre for Biologics Research, Biologics and Genetic Therapies Directorate, Health Canada, Ottawa, ON, Canada. [7]Institució Catalana de Reserca i Estudis Avançacts (ICREA). [8]Josep Carreras Leukemia Research Institute and Cell Therapy Program, Facultat de Medicina, Barcelona University, Barcelona, Spain.

Authorship contributions: R.Ru & A.A: development of methodology, acquisition, analysis and interpretation of data and manuscript writing. **L.M-C:** acquisition, analysis and interpretation of data. **C.S, J.T, L.S, A.A, I.C, F.M & M.R-M:** analysis and interpretation of data. **J.G-C:** development of methodology**,** conception and design, analysis and interpretation of data, financial support and manuscript writing. **P.M & R.Ro:** Conception and design, analysis and interpretation of data, financial support and manuscript writing. The manuscript has been seen and approved by **all authors.**

§**Correspondence should be addressed to:**
Rene Rodriguez PhD
Hospital Universitario Central de Asturias and Instituto Universitario de Oncología del Principado de Asturias, Laboratorio 2 ORL–IUOPA, 33006 Oviedo, SPAIN.
Phone: 00 34 985 108000 (ext 38524) / Fax: 00 34 985108015
Email: renerg@ficyt.es

Pablo Menendez PhD MBA
Josep Carreras Leukemia Research Institute. Facultat de Medicina. University of Barcelona. Carrer de Casanova 143. 08036. Barcelona. Spain.
Phone: 00 34 935572810 / Fax: 00 34 933231751
Email: pmenendez@carrerasresearch.org

*These authors contributed equally to this work
§Pablo Menendez and Rene Rodriguez share senior authorship

Acknowledgments: this work was supported by the Instituto de Salud Carlos III/Fondos FEDER [PI10/00449 to P.M, PI11/00377FIS to J.G-C, CP11/00024 to R.Ro, Tercel (RD12/0019/0006) and RTICC (RD12/0036/0015 and RD12/0036/0027)]; the Junta de Andalucia/FEDER (P08-CTS-3678 to P.M), the MINECO (PLE-2009-0111 to P.M), The Spanish Association Against Cancer (Junta Provincial de Albacete-CI110023 to P.M), Grupo Español de Investigación en Sarcomas

(beca J.M. Buesa-2012 to R.Ro.), Obra Social Cajastur-IUOPA, EuroNanomed ERA-NET initiative (REBONE project; PI10/02985FIS to J.G-C), Comunidad de Madrid (CellCAM; P2010/BMD-2420 to J.G-C) and Health Canada (H4084-112281 to P.M, R.Ro, and M.R-M). R.Ro and A.A. are supported respectively by the Miguel Servet and Sara Borrell programs of the ISCIII/FEDER. R.Ru was supported by a fellowship of the ISCIII/FEDER. P.M is an ICREA Professor supported by the Generalitat of Catalunya.

Conflict of interest disclosures: The authors reported no potential conflicts of interest.

Keywords: Mesenchymal stem cells; osteosarcoma; bone; tumoral microenvironment; p53; Rb; BMP-2, WNT signaling.

Word count: 5061

ABSTRACT

The cellular microenvironment plays a relevant role in cancer development. We have reported that mesenchymal stromal/stem cells (MSCs) deficient for p53 alone or together with RB ($p53^{-/-}$ $RB^{-/-}$) originate leiomyosarcoma after subcutaneous (s.c.) inoculation. Here, we show that intra-bone or periosteal inoculation of $p53^{-/-}$ or $p53^{-/-}RB^{-/-}$ bone marrow- (BM) or adipose tissue-derived MSCs (ASCs) originated metastatic osteoblastic osteosarcoma (OS). To assess the contribution of bone environment factors to OS development, we analyzed the effect of the osteoinductive factor bone morphogenetic protein-2 (BMP-2) and calcified substrates on $p53^{-/-}RB^{-/-}$ MSCs. We show that BMP-2 upregulates the expression of osteogenic markers in a WNT signaling-dependent manner. In addition, the s.c. co-infusion of $p53^{-/-}RB^{-/-}$ MSCs together with BMP-2 resulted in appearance of tumoral osteoid areas. Likewise, when $p53^{-/-}RB^{-/-}$ MSCs were inoculated embedded in a calcified ceramic scaffold composed by hydroxyapatite and tricalciumphosphate (HA/TCP), tumoral bone formation was observed in the surroundings of the HA/TCP scaffold. Moreover, the addition of BMP-2 to the ceramic/MSC implants further increased the tumoral osteoid matrix. Together, these data indicate that bone microenvironment signals are essential to drive OS development.

INTRODUCTION

Over the last years, MSCs and/or MSC-derived lineage-specific progenitors have been proposed as the cell of origin for certain soft tissue sarcomas (STS) and primary bone sarcomas [1-4]. Within bone sarcomas, OS constitutes the most frequent one comprising ~20% of new diagnosis [5, 6]. The prevalence of OS correlates with skeletal growth presenting the main incidence peak in the second decade of life. OS is also relatively common in elderly adults and is often preceded by certain genetic predispositions such as the Li-Fraumeni syndrome or hereditary retinoblastoma [7-9]. These syndromes are caused by germline mutations of P53 and RB, respectively, and importantly, mutations in p53 and/or RB pathways are also common in sporadic OS, suggesting a relevant role for the alterations in these tumor suppressor genes in the OS development [7, 10, 11]. P53 and RB play a key role in the regulation of MSC differentiation pathways. Thus, p53 activation suppresses osteoblast differentiation by inhibiting the expression of Runx2 [12]. Conversely, p53 deletion accelerates osteoblastic differentiation while impairing osteocyte terminal maturation [13]. P53 also inhibits the adipogenic and smooth muscle differentiation programs by down-regulating PPARγ and MYOCD, respectively [14]. On the other hand, RB was reported to regulate mesenchymal differentiation along different mesenchymal lineages, including osteoblastic, adipogenic and myogenic through the transcriptional regulation of several lineage-specific transcription factors [15-18].

The development of p53 and/or RB-deficient mesenchymal lineage-specific mouse models supported the link between these tumor suppressors and OS [9]. Thus, the inactivation of p53 alone or in combination with RB in the osteoblastic lineage led to OS development in nearly 100% of mice [19, 20]. Similarly, the inactivation of RB and/or p53 in early mesenchymal progenitors of embryonic limb buds resulted in sarcoma development presenting a lower incidence of OS (60% in $p53^{-/-}$ mice and 20-30% in $p53^{-/-}RB^{-/-}$ mice) and an increased incidence of poorly differentiated STS [15, 21]. Additionally, we have studied the role of p53 and/or RB deficiency in

sarcomagenesis using *ex vivo* cultures of MSCs and have reported that $p53^{-/-}$ and $p53^{-/-}RB^{-/-}$ adipose derived-MSCs (ASCs) or bone marrow derived-MSCs (BM-MSCs) give rise to leiomyosarcoma-like tumors when injected s.c. in immunodeficient mice [22, 23]. Nevertheless, when BM-MSCs were differentiated along the osteoblastic lineage before Cre-mediated deletion of p53 and RB, they generated OS-like tumors upon s.c injection in immunodeficient mice, evidencing that the stage of differentiation seems to contribute to the sarcoma phenotype [23]. However, the possibility that undifferentiated MSCs might also represent the cell of origin for OS under the influence of certain bone microenvironment signals cannot be ruled out.

BMPs are instrumental in the regulation of osteogenic differentiation of MSCs during development [24]. BMP signaling transduction through SMAD-dependent and SMAD-independent pathways converges at the RUNX2 gene to control osteogenic differentiation [24]. Within BMPs, BMP-2 is an osteoinductive morphogen abundant in the bone extracellular matrix with proven activity on MSCs, and defined roles in bone formation processes [24, 25]. BMP-2 is extensively expressed in the growth plate, and its inhibition prevents osteogenic differentiation [26, 27]. Likewise, the loss of BMP-2 in limb bud mesenchymal tissues leads to the inability to repair post natal fractures [28] and the co-inactivation of both BMP-2 and BMP-4 results in severe osteogenesis impairment [29]. Conversely, a short term expression of the BMP-2 is necessary and sufficient to induce bone formation [30]. These results evidence the central role that BMP-2 plays in post natal bone growth and bone fracture healing and support its clinical use to stimulate new bone formation [31, 32].

Besides osteogenic morphogens such as BMP-2, calcified extracellular matrix is another singular environmental factor that plays a role in bone tissues. Endosteal microenvironment is a well-defined MSC niche where cells adhere to calcified substrates and are highly exposed to calcium ions. This is the rationale for many bone regeneration strategies using calcium phosphate biomaterials, such as bioactive HA/TCP ceramic powders, as scaffolds to support the growth of MSCs in the repair of damaged bone tissue [33-35]. Likewise, OS cell lines grown onto ceramic

materials showed an osteoblastic phenotype and a modified cytokine expression pattern as compared to plastic-adhered cultures [36].

Here, we wanted to assess whether the bone microenvironment is capable of redirecting the sarcomagenesis potential/phenotype of undifferentiated $p53^{-/-}$ and/or $p53^{-/-}RB^{-/-}$ MSCs. Our data show that p53 or p53/RB deficiency in undifferentiated BM-MSCs/ASCs promotes metastatic osteoblastic OS development upon intra-bone or periosteal orthotopic transplantation while leiomysarcoma-like tumors are developed after s.c. inoculation of these cells [22, 23]. Furthermore, s.c inoculation of $p53^{-/-}RB^{-/-}$ BM-MSCs/ASCs together with BMP-2 or embedded into ceramic implants containing HA/TCP resulted in an increased appearance of osteogenic differentiated areas within the tumor. Overall, these data indicate that bone microenvironment signals are essential to drive *in vivo* the osteogenic differentiation of transformed p53- or p53/RB-deficient BM-MSCs/ASCs, eventually promoting OS development.

MATERIALS AND METHODS

Generation of mutant MSCs and cell culture

Wt, $p53^{-/-}$, $RB^{-/-}$ and $p53^{-/-}RB^{-/-}$ BM-MSCs and ASCs were obtained and cultured as previously described from FVB background mice bearing alleles for either p53, RB or both genes flanked by loxP sites [22, 23]. Mutant MSCs were generated by excision of the LoxP-flanked sequences by infection with adenoviral vectors expressing the Cre-recombinase. Successful gene knockdown was confirmed by genomic PCR. MSCs were tagged with GFP as reporter gene using the pWPI lentiviral vector (Addgene, 12254). The production of the viral particles, and the transduction of MSC cultures was performed as previously described [37]. Only early-passage (p5 to p15) MSCs were used in downstream experiments. Saos-2 cells were obtained from de ATCC and cultured as previously described [38]. Saos-2 conditioned medium was collected after 4 days of confluent culture and was concentrated using Amicon Ultra Centrifugal filters (Millipore, Billerica, MA) before being added to the MSC cultures.

In vivo tumorogenic assays

Ectopic and orthotopic inoculations:

NOD/SCID-IL2γ$R^{-/-}$ (NSG) immunodeficient mice were obtained from Jackson Laboratories (Bar Harbor, ME). Mice were housed under specific pathogen-free conditions, fed *ad libitum* and maintained under veterinary care according to animal welfare guidelines. Eight to ten weeks old mice were inoculated either subcutaneously (s.c.), intra-bone (i.b.) or periosteally (p.). Prior to inoculation, cells were resuspended in PBS with or without 20 μg/ml BMP-2 (Noricum, Madrid, Spain) and filtered through a 70 μm nylon filter. For s.c. inoculation, 5 x 10^6 cells/mouse were injected under the skin in the flank of the mice. For the i.b. inoculation, mice were anesthetized with isoflurane and the leg was bent 90^o in order to drill the tip of the tibia with a 25G needle before cell inoculation (2.5 x 10^5 cells/mouse) using a 27G needle. Mice were treated

with Buprenorphine:Carprofen (0.1:5 mg/kg) right after inoculation and then 24h and 48h after. For p. inoculation, mice were anesthetized by intraperitoneal injection of xylacine (Rompun, Bayer) and ketamine (Imalgene 1000, Merial). Then, 1 x 10^6 cells/mouse were loaded in a syringe with a 26G needle which was inserted from proximal to distal site of the leg until it reached the diaphysis of tibia and following the tibial crest. Bone surface was scraped with the needle and cells were deposited in the periosteal space. Animals were sacrificed when the tumors reached approximately 1 cm^3 or six months after inoculation. All animal research protocols were approved by the corresponding Institutional Animal Research Ethical Committees.

Ceramic Implant preparation and implantation:

40 mg of HA/TCP powder (Biomatlante, Vigneux de Bretagne, France), washed previously with 1 ml of DMEM medium, were mixed with 1 x 10^6 MSCs in 1 ml of DMEM medium. The mixture was spun down (1000 rpm, 5 minutes) and the ceramic/MSCs mix was cultured overnight. Then, the culture medium was removed and 35µl of a 1µg/µl solution of BMP-2 reconstituted in culture medium, 30 µl of thrombin (Sigma, St. Louis, MO) reconstituted in 2% $CaCl_2$ and 30 µl of fibrinogen (Sigma) reconstituted in water were added to the ceramic/MSC mix. Finally, the implant mixture was allowed to solidify for 30 minutes in cell culture conditions. For the s.c. implantation, mice were anesthetized by intraperitoneal injection of xylacine and ketamine and the surgical areas were shaved and sterilised with 70% alcohol. Next, a dorsal incision in the skin was made and a pocket under cutaneous tissue was created. When the implant was stably placed the wound was sutured.

µCT analysis

Formol fixed samples were imaged in a µCT system (eXplore Vista, GE Healthcare, Pittsburgh, PA), with an X-ray tube voltage of 50 kV and a current of 200 µA. The scanning angular rotation was 180°, the angular increment 0.40° and the voxel resolution 50 µm. Data sets were

reconstructed and segmented into binary images and 3D surface reconstructions were made using MicroView ABA 2.2 software (GE Healthcare).

Histological processing and immunohistochemistry.

Tumor samples were fixed in formol and when necessary decalcified with 4% clorhidric acid/4% formic acid for 3 days before being embedded in paraffin, cut into 4-µm sections, and subjected to Hematoxylin and eosin (H&E) staining, Masson's tricrome (M-T) staining or immunohistochemistry for GFP detection. For M-T staining, deparafined samples were stained with Harris´ hemotoxilin for 10 min. Then, samples were washed for 5 min in water, stained with Fuccina ponceau dye for 5 min, and washed with phosphomolibdic acid. Next, samples were stained with methyl violate dye for 5 min, and finally, dehydrated with increasing alcohols and xilol. Immunohistochemistry against GFP and Ki67 was performed using specific anti-GFP (1:100, Invitrogen, Paisley, UK) and anti-Ki67 (1:100, Thermo Scientific, Waltham, MA) antibodies respectively, and a secondary anti-rabbit biotinylated antibody (1:500, Jackson ImmunoResearch, Newmarket, UK). Tumor grade was analyzed in H&E stained preparations using the French Federation of Comprehensive Cancer Centers (FNCLCC) grading system [39].

Flow Cytometry and Cell Sorting

The immunophenotype of MSCs and tumor cell lines was determined by flow cytometry using fluorochrome-conjugated monoclonal antibodies anti-Sca-1, CD11b, CD14, CD29, CD44, and CD45 (BD Bioscience, Franklin Lakes, NJ) as described [37].

Genomic PCR

Total DNA was extracted using the DNeasy Kit (Qiagen, Valencia, CA). 200 ng of DNA were used for each PCR reaction. PCR conditions were as follow: pre-denaturation at 94ºC for 5 min followed by 29 cycles of denaturation at 94ºC for 30 sec, annealing at 62ºC (for p53), 60ºC (for

RB) or 67ºC (for β-actin) for 30 sec and extension at 72ºC for 50 sec. Primer sequences used are shown in **Table S1**.

Quantitative PCR

Total RNA was extracted from transformed MSCs and tumor-derived cell lines. cDNA synthesis was performed using the First-strand cDNA Synthesis Kit (GE Healthcare) and the expression of relevant genes was assessed by RT-qPCR using SYBR Green PCR Kit (Qiagen) in untreated cells or in cells treated with BMP-2 (4µg/ml), BMP-2 + DMH1 (R&D systems, Minneapolis, MN) (0.5µM) or BMP-2 + DKK1 (R&D systems, Minneapolis, MN) (0.1µg/ml). β-actin was used as a housekeeping gene. The following PCR conditions were used: 5 min at 94ºC, 35 cycles of 30 sec at 94ºC followed by 50 sec at 60ºC and 50 sec at 72ºC and a final extension of 10 min at 72ºC. Primer sequences are shown in **Table S1**. Statistical significance of the gene expression levels was analyzed using the Student's t-test.

Western Blot

Whole cell protein extraction and western blot analysis were done as previously described [40] using anti-β-catenin (1:1000, BD bioscience) and anti-β-Actin (1:20.000, Sigma, St. Louis, MO) primary antibodies.

Measurement of alkaline phosphatase activity

The activity of alkaline phosphatase (ALP) was evaluated through a colorimetric assay using cell lysates prepared after a 7-day treatment in the indicated conditions as previously described [41]. Total cellular protein content of cell lysates was determined using a Bradford assay (BioRad, Hercules, CA) and the ALP activity (O.D. 405 nm) per µg of total protein was represented.

RESULTS

Bone environment signals redirect the sarcomagenic phenotype of $p53^{-/-}$ and $p53^{-/-}RB^{-/-}$ MSCs towards OS development.

We have previously reported that Cre-mediated depletion p53 and/or Rb in $p53^{loxP/loxP}$, $RB^{loxP/loxP}$, and $p53^{loxP/loxP}RB^{loxP/loxP}$ MSCs caused a significant increase in the proliferation and life span of mutant MSCs, and that p53- and p53/RB-deficient BM-MSCs or ASCs originate leiomyosarcoma-like tumors after s.c. inoculation into immunodeficient mice [22, 23]. We hypothesized that the bone microenvironment may play a role in regulating the osteogenic differentiation of transformed MSCs, and that intra-bone (orthotopic) delivery of these transformed MSCs may impose an OS phenotype. To address this, green fluorescence protein (GFP)-tagged cultures of wild type (wt), $p53^{-/-}$, $RB^{-/-}$ and $p53^{-/-}RB^{-/-}$ BM-MSCs and ASCs [22, 23] were inoculated intra-tibia into NSG immunodeficient mice. As previously seen in s.c. inoculation experiments, only $p53^{-/-}$ and $p53^{-/-}$ $RB^{-/-}$ BM-MSCs or ASCs developed tumors *in vivo* **(Table 1)**. $p53^{-/-}RB^{-/-}$ MSCs displayed a higher tumor incidence and shorter latency than $p53^{-/-}$ MSCs **(Table 1)**. Micro Computered Tomography (μ-CT) analysis revealed the formation of tumors resembling human OS radiographic features in the tibia of mice inoculated with $p53^{-/-}RB^{-/-}$ BM-MSCs or ASCs **(Fig. 1A)**. These tumors displayed changes in the cortical bone intensity and mineralized osteoid both inside and outside of the bone [5]. H&E or M-T staining of tumors **(Fig. 1B and Fig. S1)** confirmed their resemblance with human OS **(Fig. S2)**, including the presence of extensive areas of osteid matrix formed by spindle or polyhedral tumoral cells both inside **(Fig. 1B-i & ii)** and outside the host bone marrow cavity **(Fig. 1B-i, iii & iv).** These osteoid areas commonly display a lacy pattern, typical of osteoblastic OS, and are mainly formed by GFP+ cells, confirming their tumoral origin **(Fig. 1B-iv-v)**. Likewise, the classical periosteal reaction to tumoral cells is also observed. The new formed reactive bone usually displayed the typical “sunburst” appearance **(Fig. 1B-i & v and Fig. S1A-iii)**. Although the osteoblastic component was predominant, tumors derived from both p53- and

p53RB-deficient BM-MSCs and ACSs also displayed areas of tumoral condroblastic differentiation **(Fig. 1B-vi)**. Importantly, all these OS-related features were less evident or completely lost in the areas of the tumor distant from the recipient bone. Tumoral areas far from the host bone displayed a pathology resembling undifferentiated sarcomas mainly composed by interlacing fascicles of spindle cells, similar to the leiomyosarcoma-like tumors generated by these MSCs upon s.c. inoculation **(Fig. 1B-vii).** This indicates that the host bone environment seems to play an active role in programming the oncogenic potential/phenotype of transformed MSCs. The grading of a cohort of the tumors applying a three-grade system commonly used for sarcomas classification (FNCLCC system) [39], suggests that tumors derived from $p53^{-/-}$ or $p53^{-/-}RB^{-/-}$ BM-MSCs present higher mitotic counts, and therefore higher grade than tumors derived from the corresponding ASC genotypes **(Table S2)**.

The malignant nature of OS is evidenced by the appearance of metastasis. In our model, we detected GFP+ cells colonizing and metastasizing in lungs, spleen and heart of different mice **(Fig. 1C and Fig. S3)**. Importantly, all these distant metastasis presented extensive mineralized osteoblastic areas further evidencing the OS nature of the primary tumor **(Fig. S3)**.

Although OS usually arises in the marrow cavity of long tubular bones, it also may arise on the surface of the bones [5]. Therefore, to investigate other orthotopic bone environments, GFP-tagged $p53^{-/-}$ and $p53^{-/-}RB^{-/-}$ BM-MSCs/ASCs were inoculated in the periosteal space of the tibia of immunodeficient mice. $p53^{-/-}RB^{-/-}$ MSCs also developed tumors with a shorter latency than $p53^{-/-}$ MSCs **(Table 1)**. These tumors showed similar radiological **(Fig. 2A and Fig. S4)** and histological **(Fig. 2B-C)** OS-like features to those intra-tibia-formed tumors. Tumoral osteoid/chondroid areas adjacent to both the outer and the inner sides of the bone were evidenced by μ-CT analysis **(Fig. 2A and Fig. S4)** and H&E or M-T staining **(Fig. 2B-C)**. These newly formed osteoid/chondroid areas comprises GFP+ cells confirming a tumoral MSC origin **(Fig. 2B-iii and 2C-iii)**.

To further characterize these experimentally-induced OS, primary tumors derived from $p53^{-/-}$ and $p53^{-/-}RB^{-/-}$ BM-MSCs as well as $p53^{-/-}$ ASCs were harvested, disaggregated and placed back in MSC culture conditions to establish immortalized cell lines (TIB-BM-p53#1, TIB-BM-p53RB#1 to #3 and TIB-ASC-p53#1 to #3). As expected, these tumor cell lines remained deficient for p53 and RB **(Fig. 3A)** and displayed identical immunophenotype than their parental MSCs **(Fig. 3B and Fig S5)** [22, 23]. Next, to further confirm the OS diagnosis of tumors at the molecular level, we analyzed the expression of several early (BMP-4 and Osterix) and late (Osteopontin and Osteocalcin) osteogenic markers in two TIB-BM-p53RB cell lines **(Fig. 3C)** and two TIB-ASC-p53 cell lines **(Fig. 3D)**. All these osteogenic markers were up-regulated in the TIB-BM-p53RB cell lines as compared to the parental BM-MSCs (BM-MSC-$p53^{loxP/loxP}RB^{loxP/loxP}$), and to a cell line derived from a leiomyosarcoma-like tumor formed upon s.c. inoculation of $p53^{-/-}RB^{-/-}$ BM-MSCs (T-BM- p53RB) **(Fig. 3C)**. Similarly, these osteogenic markers were partially up-regulated in TIB-ASC-p53 cell lines as compared to the parental ASCs (ASC-$p53^{loxP/loxP}$) **(Fig. 3D)**. Together, these data indicate that environment signals provided by the bone milieu are able to redirect towards an OS development the otherwise leiomyosarcoma tumorogenic potential of p53/RB-deficient MSCs.

BMP-2 promotes osteogenic differentiation through the activation of WNT signaling and promotes OS development from $p53^{-/-}RB^{-}$ MSCs with no need of orthotopic inoculation.

We have demonstrated that signals from the bone milieu induce *in vivo* osteogenic differentiation of transformed $p53^{-/-}RB^{-/-}$ BM-MSCs/ASCs and OS development. We next attempted to investigate the contribution of individual osteogenic factors. We first studied the response of $p53^{-/-}$ $RB^{-/-}$ BM-MSCs/ASCs to treatment with media conditioned by confluent cultures of Saos-2 cells, a human osteosarcoma cell line with high osteoinductive ability [38]. We found that p53-/-RB-/- BM-MSCs/ASCs treated with Saos-2 conditioned medium displayed a significant increase in the osteoblastic-related ALP activity **(Fig. S6)**. Since Saos-2 cells osteoinductive ability is highly

dependent on the expression of osteogenic BMPs [38], we analyzed whether BMP-2 confers osteogenic differentiation potential to $p53^{-/-}RB^{-/-}$ BM-MSCs. BMP-2 was able to induce the expression of early (Osterix and ALP) and late (Osteocalcin) osteogenic markers which was reversed by DMH1, a selective inhibitor of the type I BMP receptors (BMPR-I) [42] that mediate the BMP-2-induced osteblastic signals in MSCs [43] **(Fig. 4A).**

It was reported that the pro-osteogenic effect of BMP-2 on pre-osteoblastic cells is mediated through the BMP-2-induced activation of WNT signaling [44]. We thus investigated whether WNT signaling is also relevant in the BMP-2-induced osteogenic differentiation of transformed MSCs. We found that treatment of $p53^{-/-}RB^{-/-}$ BM-MSCs with BMP-2 resulted in a 20-fold upregulation of the canonical WNT signaling activator WNT3A that was fully reversed by the BMPR-I inhibitor DMH1 **(Fig. 4B)**. Likewise, BMP2 treatment increased intracellular levels of key WNT signaling mediator β-catenin **(Fig. 4C)**. The WNT signaling inhibitor dickkopf 1 (DKK1) prevented β-catenin accumulation **(Fig. 4C)** and was able to almost completely block the BMP-2-induced expression of osteogenic markers **(Fig. 4A)** suggesting that BMP-2 induces osteogenic differentiation of transformed MSCs through the regulation of WNT signaling.

After confirming the osteogenic effect of BMP-2 *in vitro*, we studied whether BMP-2 also confers *in vivo* osteogenic differentiation potential and promotes OS development from GFP-tagged $p53^{-/-}$ $RB^{-/-}$ BM-MSCs/ASCs delivered via s.c. into immunodeficient mice. Both control- and BMP-2-treated $p53^{-/-}RB^{-/-}$ BM-MSCs and ASCs developed tumors with similar penetrance and latency **(Table 2)**. As previously reported [22, 23], tumors developed from control-treated $p53^{-/-}RB^{-/-}$ BM-MSCs/ASCs resembled leiomyosarcomas, and did not show evidence of osteogenic differentiation **(Fig. 4D)**. However, tumors developed from both $p53^{-/-}RB^{-/-}$ BM-MSCs and $p53^{-/-}$ $RB^{-/-}$ ASCs s.c. inoculated with BMP-2 displayed extended areas of osteoid matrix **(Fig. 4D)**. Importantly, these bone-forming areas were GFP+, confirming that they developed from the BMP-2-stimulated $p53^{-/-}RB^{-/-}$ MSCs **(Fig. 4D)**. These data support the ability of BMP-2 to induce

osteogenic differentiation of transformed MSCs *in vivo,* and to contribute to the acquisition of the OS phenotype in an ectopic (s.c.) environment.

Calcified substrates induce *in vivo* osteogenic differentiation of $p53^{-/-}RB^{-/-}$ MSCs and synergistically cooperate with BMP-2 in OS development.

Apart from individual osteogenic factors present in the bone milieu, like BMP-2, the calcified extracellular matrix is another key environmental factor supposed to play a role in osteogenic differentiation [33, 34]. To test the osteoinductive ability of the calcified extracellular matrix alone or in combination with BMP-2, we prepared pellets of $p53^{-/-}RB^{-/-}$ BM-MSCs/ASCs containing or not HA/TCP as calcified substrate and cultured them in the presence or absence of BMP-2. Consistent with the BMP-2-induced expression of the ALP gene **(Fig 4A)**, we observed an increase in ALP activity in BMP-2 treated $p53^{-/-}RB^{-/-}$ BM-MSCs/ASCs **(Fig 5A)**. On the other hand, cells embedded in HA/TCP alone displayed only a modest gain in ALP activity, although the combination of both HA/TCP ceramic and BMP-2 synergistically increased ALP activity **(Fig 5A)**. To test the role of calcified substrates and BMP-2 combination in OS development *in vivo*, we devised ceramic implants composed by HA/TCP, GFP-expressing $p53^{-/-}RB^{-/-}$ BM-MSCs/ASCs and a fibrin coating to facilitate their s.c. implantation into immunodeficient mice **(Fig. 5B)**. Both control (culture medium) and BMP-2 loaded implants developed tumors with similar latencies **(Table 2)**. Importantly, tumors developed in the absence of BMP-2 showed small areas of osteogenic differentiation only surrounding the ceramic material **(Fig. 5C-D).** However, when BMP-2 was incorporated to the ceramic-fibrin structure, tumors containing large areas of GFP+ tumorogenic osteoid matrix, spread throughout the tumor and resembling the lace-like pattern typical of human OS, were developed **(Fig. 5C-D)**. All tumors showed abundant proliferating cells (nuclear Ki67 staining) both in undifferentiated areas and in the surroundings of osteoid-differentiated areas and the presence of BMP-2 or calcified substrates did not seem to influence the proliferation index **(Fig S7)**.

These results suggest a relevant role for bone milieu signals in the development of the OS phenotype from $p53^{-/-}RB^{-/-}$ transformed MSCs. This HA/TCP-based ceramic/fibrin bone-like environment model represents a powerful system for testing potential individual factors/molecules involved in OS pathogenesis as well as novel therapeutic compounds.

DISCUSSION

Cancer-specific hallmark oncogenic hits must arise in the appropriate target cell (the so-called tumor initiating cell, TIC) in order to initiate an oncogenic process [45]. However, increasing evidence supports a relevant role of the cellular microenvironment in regulating both stem cell fate and cancer cell growth [46-48]. Cell-cell contact interactions and paracrine soluble factors may influence the tumor phenotype and evolution [45, 48]. Thus, *in vivo* models capable of integrating both the nature of the target cell for transformation, the underlying oncogenic lesions, and the influence of the microenvironment will constitute a valuable model to study tumor biology and to assess potential novel therapeutic approaches [48].

Solid evidence indicates that MSCs and/or MSC-derived progenitors represent the TIC for human sarcomas [1-4]. Likewise, normal, non-malignant MSC-like cells have been isolated at high frequencies from primary OS samples, suggesting that normal MSCs could be recruited to the microenvironment of OS and play a role in the development of the disease [49]. p53 and RB are master cell cycle regulators related with MSC differentiation [12-17], and loss-of-function mutations in p53 and/or RB are common in sarcomas, especially in OS, suggesting a relevant role for p53/RB deficiency as OS-driving mutations [6, 10, 11]. We have previously reported that p53 and RB inactivation in undifferentiated BM-MSCs or ASCs induces leiomyosarcoma upon s.c inoculation into immunodeficient mice [22, 23]. Conversely, p53 and RB inactivation in BM-MSC-derived osteogenic progenitors efficiently promoted the development of OS upon s.c. inoculation, whereas $p53^{-/-}RB^{-/-}$ ASC-derived osteogenic progenitors did not display tumorogenic potential [23]. These data indicate that the differentiation stage of BM-MSCs may impose the tumor phenotype. However, mouse models in which p53/RB were mutated in early mesenchymal progenitors of embryonic limb buds also developed OS [15, 21], suggesting that undifferentiated MSCs could also constitute the cell of origin for OS under certain osteogenic-inductive signals. In this regard, the expression of c-MYC in $p16^{INK4A-/-}p19^{ARF-/-}$ undifferentiated BM-MSCs resulted in

OS development [50]. Additionally, similar gene expression signatures were found between human OS samples and undifferentiated MSCs or osteogenic-committed MSCs [51], suggesting that OS may develop in osteogenic progenitors or in undifferentiated MSCs.

To address whether the bone environment influences the *in vivo* differentiation and the sarcomagenic potential of transformed MSCs, $p53^{-/-}$ and $p53^{-/-}RB^{-/-}$ BM-MSCs and ASCs were inoculated either intra-bone or in periosteum. Orthotopic inoculation of these transformed undifferentiated MSCs consistently generated osteoblastic OS displaying human OS radiographic and histological features, including extensive areas of tumoral osteoid matrix. The osteogenic ability of the transformed MSCs was further evidenced by their infiltration (metastasis presenting osteoid areas) in lung, spleen and heart. Moreover, *ex vivo* tumoral cell lines derived from primary tumors displayed up-regulation of early and late osteogenic markers. Together, these data demonstrate that bone environment signals play a role in osteogenic differentiation and sarcomagenesis by defining the sarcoma phenotype regardless the source of the MSCs. Therefore, either BM-MSC-derived osteogenic progenitors or undifferentiated BM-MSCs/ASCs may represent of OS-TIC under the proper microenvironment signals. It might be speculated that the more differentiated the target cell for transformation is, the more differentiated the resulting OS would be [4, 6, 23]. Notably, the histological OS features became less evident in areas distant from the host bone, further highlighting the role of microenvironment signals in osteogenic differentiation. In line with this, a recent characterization of 19 OS cell lines found that half of them were unable to generate tumors after ectopic inoculation into immunodeficient mice and the remaining cell lines generated tumors classified as high grade sarcomas displaying only a discrete osteogenic differentiation [52].

We have previously reported that gene expression profiling of BM-MSCs differentiated along the osteoblastic lineage before Cre-mediated deletion of p53 and RB, which generate OS after s.c. inoculation into inmunedeficient mice, showed alterations in several signaling pathways related to

osteogenic differentiation and OS development, like those controlled by WNT (including the regulation mediated by WNT3A), calcium and BMPs [23]. Therefore, we next wanted to study the individual contribution of master bone microenvironment factors such as BMP-2, WNT signaling and calcified substrates to OS development. BMP-2 is expressed in human OS [53], and its role in OS development has been addressed in OS cell lines but not in primary transformed MSCs. We show that BMP-2 treatment enhances the expression of osteogenic markers in transformed MSCs. Likewise, BMP-2 is able to effectively induce *in vivo* osteogenic differentiation and OS development upon ectopic s.c inoculation of $p53^{-/-}RB^{-/-}$ BM-MSCs and ASCs without significant differences in tumor latency, thus mimicking the effects observed upon orthotopic inoculation of $p53^{-/-}RB^{-/-}$ BM-MSCs/ASCs. Previous work on OS cell lines revealed controversial effects of BMP-2 on osteogenic differentiation and tumor growth. It has been reported that BMP-2 failed to induce bone formation from human OS cell lines that harbor differentiation defects and instead efficiently promote tumor growth [54]. Conversely, it has been shown that BMP-2 treatment of a TIC population isolated from human OS cell lines induced the upregulation of terminal osteogenic markers inhibiting their tumorogenic potential [55]. These controversial data on genomically unstable transformed OS cell lines pinpoints the need to study differentiation and transformation processes using primary MSCs harboring defined oncogenic lesions.

A previous report has shown that BMP-2 controls important features of MSC osteoblastic differentiation though the autocrine activation of WNT ligands like WNT1 and WNT3A [44]. Likewise, it was suggested that osteoblasts exert a direct control of osteogenic lineage commitment of mesenchymal progenitors through WNT singnaling-activating ligands, including WNT3A which is able to stimulate osteogenesis [56]. Similarly, we show that BMP-2 induces the expression of WNT3A and the accumulation of β-catenin in transformed MSCs and that the BMP-2-induced upregulation of osteogenic markers is blocked by the WNT signaling antagonist DKK1. In addition, co-culture of transformed MSCs with and osteoinductive cell type such as Saos-2

cells [38] is able to significantly increase ALP activity. Altogether, it may be speculated that osteoinductive cell types present in the tumor microenviroment (both from host or tumoral origin) could produce osteogenic factors such as BMP-2 which in turn activated WNT signaling in transformed MSCs, thus contributing to OS phenotype development.

Calcium phosphate biomaterials, such as HA/TCP, are extensively used as a calcified scaffold to support *in vivo* the proliferation and differentiation of MSCs in degenerative or damaged osteoarticular conditions [33-35, 57]. We have recently set up a model to assess the *in vivo* differentiation potential of hMSCs based on s.c implantation into immunodeficient mice of hMSCs embedded in a fibrin-coated HA/TCP ceramic and supplemented with BMP-2 [58]. Here, we took advantage of this optimized ceramic model to analyze the effect of calcified substrates on the osteogenic differentiation and sarcomagenesis potential of $p53^{-/-}RB^{-/-}$ MSCs. Both $p53^{-/-}RB^{-/-}$ BM-MSCs and ASCs embedded in the fibrin-coated HA/TCP ceramic in the absence of BMP-2 developed tumors showing discrete areas of osteogenic differentiation surrounding the ceramic material, similar to previous studies using wt MSCs [33, 59]. However, the addition of BMP-2 displayed a synergistic effect along with HA/TCP calcified substrate resulting in OS development with extensive tumoral osteoid matrix distributed throughout the tumor. These results further highlight the importance of bone environment signals, such as calcium substrates and BMP-2, in programming the sarcomagenic potential of transformed $p53^{-/-}RB^{-/-}$ BM-MSCs/ASCs. Importantly, tumors developed from $p53^{-/-}RB^{-/-}$ BM-MSCs and ASCs in the ceramic/BMP-2 model exclusively displayed osteogenic differentiation and subsequent OS development, and no other mesenchymal tissue differentiation was found as it was observed when healthy hMSCs were inoculated [58]. This indicates that deficiency of p53 and RB predisposes BM-MSCs and ASCs towards the osteogenic lineage, thus favoring OS development.

It is worth mentioning that human cells are more resistant to undergo tumoral transformation than mouse cells, thus supporting the safety use of hMSCs in clinical aplications. In this regard,

hMSCs deficient for p53 and/or Rb failed to induce tumor formation in vivo [37, 60] suggesting that in the human setting additional cooperating mutations are needed to initiate sarcomagenesis [4, 60]. Nevertheless, it is plausible that microenvironment signals described in this work as able to influencing sarcoma formation from mMSCs are likewise relevant for modulating human sarcomagenesis.

CONCLUSION

In summary, OS development is closely linked to MSC differentiation [6] and several key factors underlie its phenotype: i) the acquisition of relevant oncogenic lesions favoring the growth advantage of tumor cells predisposed towards the osteogenic lineage; ii) the differentiation stage of MSCs towards osteogenic lineage; and iii) the influence of bone microenvironment proliferative and differentiation signals. Here, we have developed an osteoblastic OS model based on the integration of potential OS-TIC (BM-MSCs/ASCs), OS-predisposing oncogenic lesions (p53/RB deficiency), and the influence of bone microenvironment signals (calcified substrates and BMP-2). In contrast to existing OS models based on the ectopic or orthotopic inoculation of OS established cell lines into immunodeficient mice, this model is developed from the putative OS TIC, is easier to handle than orthotopic inoculations and is suitable for the study of the impact of individual milieu signals in physiological and pathological osteogenesis, eventually representing a valid model to assess the pre-clinical efficacy of novel OS therapeutic strategies.

REFERENCES

1. Abarrategi A, Marinas-Pardo L, Mirones I*, et al.* Mesenchymal niches of bone marrow in cancer. *Clin Transl Oncol* 2011;**13:**611-616.
2. Garcia-Castro J, Trigueros C, Madrenas J*, et al.* Mesenchymal stem cells and their use as cell replacement therapy and disease modelling tool. *J Cell Mol Med* 2008;**12:**2552-2565.
3. Rodriguez R, Garcia-Castro J, Trigueros C*, et al.* Multipotent mesenchymal stromal cells: clinical applications and cancer modeling. *Adv Exp Med Biol* 2012;**741:**187-205.
4. Rodriguez R, Rubio R, Menendez P. Modeling sarcomagenesis using multipotent mesenchymal stem cells. *Cell Res* 2012;**22:**62-67.
5. Klein MJ, Siegal GP. Osteosarcoma: anatomic and histologic variants. *Am J Clin Pathol* 2006;**125:**555-581.
6. Tang N, Song WX, Luo J*, et al.* Osteosarcoma development and stem cell differentiation. *Clin Orthop Relat Res* 2008;**466:**2114-2130.
7. Helman LJ, Meltzer P. Mechanisms of sarcoma development. *Nat Rev Cancer* 2003;**3:**685-694.
8. Malkin D, Li FP, Strong LC*, et al.* Germ line p53 mutations in a familial syndrome of breast cancer, sarcomas, and other neoplasms. *Science* 1990;**250:**1233-1238.
9. Ng AJ, Mutsaers AJ, Baker EK*, et al.* Genetically engineered mouse models and human osteosarcoma. *Clin Sarcoma Res* 2012;**2:**19.
10. Overholtzer M, Rao PH, Favis R*, et al.* The presence of p53 mutations in human osteosarcomas correlates with high levels of genomic instability. *Proc Natl Acad Sci U S A* 2003;**100:**11547-11552.
11. Wadayama B, Toguchida J, Shimizu T*, et al.* Mutation spectrum of the retinoblastoma gene in osteosarcomas. *Cancer Res* 1994;**54:**3042-3048.
12. Lengner CJ, Steinman HA, Gagnon J*, et al.* Osteoblast differentiation and skeletal development are regulated by Mdm2-p53 signaling. *J Cell Biol* 2006;**172:**909-921.
13. Tataria M, Quarto N, Longaker MT*, et al.* Absence of the p53 tumor suppressor gene promotes osteogenesis in mesenchymal stem cells. *J Pediatr Surg* 2006;**41:**624-632; discussion 624-632.
14. Molchadsky A, Shats I, Goldfinger N*, et al.* p53 plays a role in mesenchymal differentiation programs, in a cell fate dependent manner. *PLoS One* 2008;**3:**e3707.
15. Calo E, Quintero-Estades JA, Danielian PS*, et al.* Rb regulates fate choice and lineage commitment in vivo. *Nature* 2010;**466:**1110-1114.
16. De Falco G, Comes F, Simone C. pRb: master of differentiation. Coupling irreversible cell cycle withdrawal with induction of muscle-specific transcription. *Oncogene* 2006;**25:**5244-5249.
17. Gutierrez GM, Kong E, Sabbagh Y*, et al.* Impaired bone development and increased mesenchymal progenitor cells in calvaria of RB1-/- mice. *Proc Natl Acad Sci U S A* 2008;**105:**18402-18407.
18. Thomas DM, Carty SA, Piscopo DM*, et al.* The retinoblastoma protein acts as a transcriptional coactivator required for osteogenic differentiation. *Mol Cell* 2001;**8:**303-316.
19. Berman SD, Calo E, Landman AS*, et al.* Metastatic osteosarcoma induced by inactivation of Rb and p53 in the osteoblast lineage. *Proc Natl Acad Sci U S A* 2008;**105:**11851-11856.
20. Walkley CR, Qudsi R, Sankaran VG*, et al.* Conditional mouse osteosarcoma, dependent on p53 loss and potentiated by loss of Rb, mimics the human disease. *Genes Dev* 2008;**22:**1662-1676.
21. Lin PP, Pandey MK, Jin F*, et al.* Targeted mutation of p53 and Rb in mesenchymal cells of the limb bud produces sarcomas in mice. *Carcinogenesis* 2009;**30:**1789-1795.

22. Rubio R, Garcia-Castro J, Gutierrez-Aranda I*, et al.* Deficiency in p53 but not retinoblastoma induces the transformation of mesenchymal stem cells in vitro and initiates leiomyosarcoma in vivo. *Cancer Res* 2010;**70:**4185-4194.
23. Rubio R, Gutierrez-Aranda I, Saez-Castillo AI*, et al.* The differentiation stage of p53-Rb-deficient bone marrow mesenchymal stem cells imposes the phenotype of in vivo sarcoma development. *Oncogene* 2013;**32:**4970-4980.
24. Chen G, Deng C, Li YP. TGF-beta and BMP signaling in osteoblast differentiation and bone formation. *Int J Biol Sci* 2012;**8:**272-288.
25. Luu HH, Song WX, Luo X*, et al.* Distinct roles of bone morphogenetic proteins in osteogenic differentiation of mesenchymal stem cells. *J Orthop Res* 2007;**25:**665-677.
26. Anderson HC, Hodges PT, Aguilera XM*, et al.* Bone morphogenetic protein (BMP) localization in developing human and rat growth plate, metaphysis, epiphysis, and articular cartilage. *J Histochem Cytochem* 2000;**48:**1493-1502.
27. Bais MV, Wigner N, Young M*, et al.* BMP2 is essential for post natal osteogenesis but not for recruitment of osteogenic stem cells. *Bone* 2009;**45:**254-266.
28. Tsuji K, Bandyopadhyay A, Harfe BD*, et al.* BMP2 activity, although dispensable for bone formation, is required for the initiation of fracture healing. *Nat Genet* 2006;**38:**1424-1429.
29. Bandyopadhyay A, Tsuji K, Cox K*, et al.* Genetic analysis of the roles of BMP2, BMP4, and BMP7 in limb patterning and skeletogenesis. *PLoS Genet* 2006;**2:**e216.
30. Noel D, Gazit D, Bouquet C*, et al.* Short-term BMP-2 expression is sufficient for in vivo osteochondral differentiation of mesenchymal stem cells. *Stem Cells* 2004;**22:**74-85.
31. Gautschi OP, Frey SP, Zellweger R. Bone morphogenetic proteins in clinical applications. *ANZ J Surg* 2007;**77:**626-631.
32. McKay WF, Peckham SM, Badura JM. A comprehensive clinical review of recombinant human bone morphogenetic protein-2 (INFUSE Bone Graft). *Int Orthop* 2007;**31:**729-734.
33. Barradas AM, Yuan H, van Blitterswijk CA*, et al.* Osteoinductive biomaterials: current knowledge of properties, experimental models and biological mechanisms. *Eur Cell Mater* 2011;**21:**407-429.
34. Gamie Z, Tran GT, Vyzas G*, et al.* Stem cells combined with bone graft substitutes in skeletal tissue engineering. *Expert Opin Biol Ther* 2012;**12:**713-729.
35. Hench LL, Polak JM. Third-generation biomedical materials. *Science* 2002;**295:**1014-1017.
36. Rochet N, Loubat A, Laugier JP*, et al.* Modification of gene expression induced in human osteogenic and osteosarcoma cells by culture on a biphasic calcium phosphate bone substitute. *Bone* 2003;**32:**602-610.
37. Rodriguez R, Rubio R, Gutierrez-Aranda I*, et al.* FUS-CHOP fusion protein expression coupled to p53 deficiency induces liposarcoma in mouse but not in human adipose-derived mesenchymal stem/stromal cells. *Stem Cells* 2011;**29:**179-192.
38. Raval P, Hsu HH, Anderson HC. Osteoinductive ability of confluent Saos-2 cell correlates with enhanced expression of bone morphogenetic proteins. *J Orthop Res* 1996;**14:**605-610.
39. Trojani M, Contesso G, Coindre JM*, et al.* Soft-tissue sarcomas of adults; study of pathological prognostic variables and definition of a histopathological grading system. *Int J Cancer* 1984;**33:**37-42.
40. Rodriguez R, Gagou ME, Meuth M. Apoptosis induced by replication inhibitors in Chk1-depleted cells is dependent upon the helicase cofactor Cdc45. *Cell Death Differ* 2008;**15:**889-898.
41. Abarrategi A, Moreno-Vicente C, Martinez-Vazquez FJ*, et al.* Biological properties of solid free form designed ceramic scaffolds with BMP-2: in vitro and in vivo evaluation. *PLoS One* 2012;**7:**e34117.
42. Hao J, Ho JN, Lewis JA*, et al.* In vivo structure-activity relationship study of dorsomorphin analogues identifies selective VEGF and BMP inhibitors. *ACS Chem Biol* 2010;**5:**245-253.

43. Lavery K, Swain P, Falb D*, et al.* BMP-2/4 and BMP-6/7 differentially utilize cell surface receptors to induce osteoblastic differentiation of human bone marrow-derived mesenchymal stem cells. *J Biol Chem* 2008;**283:**20948-20958.
44. Rawadi G, Vayssiere B, Dunn F*, et al.* BMP-2 controls alkaline phosphatase expression and osteoblast mineralization by a Wnt autocrine loop. *J Bone Miner Res* 2003;**18:**1842-1853.
45. Visvader JE. Cells of origin in cancer. *Nature* 2011;**469:**314-322.
46. Menendez P, Catalina P, Rodriguez R*, et al.* Bone marrow mesenchymal stem cells from infants with MLL-AF4+ acute leukemia harbor and express the MLL-AF4 fusion gene. *J Exp Med* 2009;**206:**3131-3141.
47. Pollett JB, Corsi KA, Weiss KR*, et al.* Malignant transformation of multipotent muscle-derived cells by concurrent differentiation signals. *Stem Cells* 2007;**25:**2302-2311.
48. Vermeulen L, de Sousa e Melo F, Richel DJ*, et al.* The developing cancer stem-cell model: clinical challenges and opportunities. *Lancet Oncol* 2012;**13:**e83-89.
49. Brune JC, Tormin A, Johansson MC*, et al.* Mesenchymal stromal cells from primary osteosarcoma are non-malignant and strikingly similar to their bone marrow counterparts. *Int J Cancer* 2011;**129:**319-330.
50. Shimizu T, Ishikawa T, Sugihara E*, et al.* c-MYC overexpression with loss of Ink4a/Arf transforms bone marrow stromal cells into osteosarcoma accompanied by loss of adipogenesis. *Oncogene* 2010;**29:**5687-5699.
51. Cleton-Jansen AM, Anninga JK, Briaire-de Bruijn IH*, et al.* Profiling of high-grade central osteosarcoma and its putative progenitor cells identifies tumourigenic pathways. *Br J Cancer* 2009;**101:**2064.
52. Mohseny AB, Machado I, Cai Y*, et al.* Functional characterization of osteosarcoma cell lines provides representative models to study the human disease. *Lab Invest* 2011;**91:**1195-1205.
53. Sulzbacher I, Birner P, Trieb K*, et al.* The expression of bone morphogenetic proteins in osteosarcoma and its relevance as a prognostic parameter. *J Clin Pathol* 2002;**55:**381-385.
54. Luo X, Chen J, Song WX*, et al.* Osteogenic BMPs promote tumor growth of human osteosarcomas that harbor differentiation defects. *Lab Invest* 2008;**88:**1264-1277.
55. Wang L, Park P, Zhang H*, et al.* BMP-2 inhibits the tumorigenicity of cancer stem cells in human osteosarcoma OS99-1 cell line. *Cancer Biol Ther* 2011;**11:**457-463.
56. Zhou H, Mak W, Zheng Y*, et al.* Osteoblasts directly control lineage commitment of mesenchymal progenitor cells through Wnt signaling. *J Biol Chem* 2008;**283:**1936-1945.
57. Sun H, Ye F, Wang J*, et al.* The upregulation of osteoblast marker genes in mesenchymal stem cells prove the osteoinductivity of hydroxyapatite/tricalcium phosphate biomaterial. *Transplant Proc* 2008;**40:**2645-2648.
58. Abarrategi A, Perez-Tavarez R, Rodriguez-Milla MA*, et al.* In vivo ectopic implantation model to assess human mesenchymal progenitor cell potential. *Stem Cell Rev* 2013;**9:**833-846.
59. Arinzeh TL, Tran T, McAlary J*, et al.* A comparative study of biphasic calcium phosphate ceramics for human mesenchymal stem-cell-induced bone formation. *Biomaterials* 2005;**26:**3631-3638.
60. Rodriguez R, Tornin J, Suarez C*, et al.* Expression of FUS-CHOP fusion protein in immortalized/transformed human mesenchymal stem cells drives mixoid liposarcoma formation. *Stem Cells* 2013;**31:**2061-2072.

LEGENDS TO FIGURES.

Figure 1: Development of OS upon intra-bone inoculation of p53-/- and p53-/-RB-/- BM-MSCs/ASCs. (A) Images of bone surface (isosurface; left panels) and representative sagital (right top panels) and longitudinal (right bottom panels) orthogonal images obtained by µ-CT of a control leg and legs intra-bone inoculated with p53-/-RB-/- BM-MSCs or p53-/-RB-/- ASCs. Compared to the control leg, changes in cortical bone intensity (black arrows), difuse peri-bone formation (white arrows) and intra-marrow bone formation (grey arrows) resembles human OS features in legs inoculated with transformed MSCs. **(B)** H&E staining (i-iii,vi-vii), M-T staining (iv) and GFP immuno-staining (v) of representative areas showing the main histological features of tumors arising in mice intra-bone inoculated with either p53-/- or p53-/-RB-/- BM-MSCs/ASCs (see Fig S1 for cell type/genotype classified images). **(C)** H&E staining (i-iii) and GFP immuno-staining (iv) of metastatic nodules showing osteogenic differentiation observed in the lung (i & iv), spleen (ii) and heart (iii) of mice intra-bone inoculated with p53-/-RB-/- BM-MSCs. Normal recipient bone (B), reactive bone (RB), tumoral osteogenic areas (Os), chondroblastic areas (C) and tumoral undifferentiated areas (Und) are indicated. Blue arrows indicate the presence of osteogenic tumoral cells in the BM niche, yellow arrows indicate mitotic cells and red arrows indicate the presence of osteoid matrix-forming tumoral cells. Blue lines were used to depict the border between host bone and ectopic tumor osteogenic areas.

Figure 2: Development of OS upon periosteal inoculation of p53-/- and p53-/-RB-/- BM-MSCs/ASCs. (A) Images of bone surface (isosurface; left panels) and representative sagital (right top panels) and longitudinal (right bottom panels) orthogonal images obtained by µ-CT of a control leg and legs periosteally-inoculated with p53-/- or p53-/-RB-/- BM-MSCs. Compared to the control leg, changes in cortical bone intensity (black arrows), diffuse peri-bone formation (white arrows) and intra-marrow bone formation (grey arrows) resemble human OS features in legs inoculated with transformed MSCs. **(B-C)** H&E staining (i), M-T staining (ii) and GFP immuno-

staining (iii) of tumors formed upon periosteal inoculation of GFP-expressing p53-/-RB-/- BM-MSCs **(B)** and p53-/-RB-/-ASCs **(C)**. H&E and M-T stainings are also shown as insets for non-inoculated bones (**C**; iv & v). M-T staining was used to highlight areas of bone/cartilage and GFP detection was used to distinguish host bone (GFP-) from adjacent tumor-derived osteogenic areas (GFP+). Normal recipient bone (B), normal bone marrow (BM), tumoral osteogenic areas (Os) and tumoral chondrogenic areas (C) are indicated. Blue lines were used to depict the border between host bone and ectopic tumor osteogenic areas.

Figure 3: Immortalized cell lines *ex vivo* derived from primary OS generated by tumorogenic p53- and p53/RB-deficient BM-MSCs/ASCs show a MSC phenotype and express osteogenic markers. (**A**) Genomic PCR confirming that immortalized cell lines *ex vivo*-derived from primary OS tumors formed upon intra-bone inoculation of p53-/- BM-MSCs (TIB-BM-p53), p53-/-RB-/- BM-MSCs (TIB-BM-p53RB) and p53-/- ASCs (TIB-ASC-p53) retained p53 and/or RB deficiency. **(B)** Immunophenotypic profile of the indicated tumoral cell lines analyzed by flow cytometry. Representative dot plots are shown for Sca-1, CD29, CD44, CD14, CD11b, and CD45. Empty lines represent the irrelevant isotypes. Red-filled lines display antibody-specific staining. **(C-D)** RT-qPCRs showing the up-regulation of the indicated osteogenic markers in two TIB-BM-p53RB cell lines as compared to either the original BM-MSC-p53$^{loxP/loxP}$RB$^{loxP/loxP}$ cells or to a cell line derived from a leiomyosarcoma-like tumor formed upon subcutaneous inoculation of p53-/-RB-/- BM-MSCs (T-BM-p53RB) **(C),** and in two TIB-ASC-p53 cell lines as compared to the original ASCs (ASC-p53$^{loxP/loxP}$) **(D)** [(*) P-value<0.05 vs control cells].

Figure 4. BMP-2 administration promotes osteogenic differentiation through the activation of Wnt singnaling and OS development upon subcutaneous inoculation. (A-B) RT-qPCRs showing the relative mRNA expression levels of the indicated osteogenic markers **(A)** or WNT3A **(B)** upon treatment of p53-/-RB-/- BM-MSCs with BMP-2 (4µg/ml), BMP-2 + DMH1 (0.5µM) or BMP-2 + DKK1 (0.1µg/ml) for 5 days [(*) P-value<0.05 vs control cells]. **(C)** Western blotting

showing the expression of β-catenin protein in p53-/-RB-/- BM-MSCs after a 24 hours-treatment with BMP-2 or BMP-2 + DKK1. The expression of β-actin was used as loading control. **(D)** H&E staining (i & ii), MT staining (iii) and GFP immuno-staining (iv) of tumors formed upon subcutaneous inoculation of GFP-expressing p53-/-RB-/- BM-MSCs or p53-/-RB-/- ASCs implanted without (i) or with 40 µg of BMP-2 (ii-iv). Tumoral osteogenic areas (Os) are indicated.

Figure 5. A ceramic bone-like environment model allows testing of individual bone factors involved in OS development. (A) ALP activity per µg of protein in lysates of $p53^{-/-}RB^{-/-}$ BM-MSCs/ASCs pellets containing or not HA/TCP after a 7-day treatment with or without BMP-2 (4µg/ml) as indicated [(*) P-value<0.05 vs control cells; (§) P-value<0.05 vs BMP-2 treated cells]. **(B)** 40 mg of ceramic-fibrin based implants were used as carrier of tumoral cells and BMP-2. A representative implant (i) and a schematic sequence of the inoculation process (ii-v) are shown. **(C-D)** H&E staining (i-ii), M-T staining (iii-iv) and GFP immuno-staining (v) of tumors formed upon subcutaneous inoculation of ceramic implants containing GFP-expressing p53-/-RB-/- BM-MSCs **(C)** or p53-/-RB-/- ASCs **(D)** with or without 40 µg of BMP-2 as indicated. Ceramic pieces (Cer) and tumoral osteogenic areas (Os) are indicated.

LEGENDS TO SUPPLEMENTARY FIGURES.

Figure S1: Development of OS upon intra-bone inoculation of $p53^{-/-}$ and $RB^{-/-}p53^{-/-}$ BM-MSCs/ASCs. H&E staining of tumors arising in mice intra-bone inoculated with either $p53^{-/-}$ BM-MSCs **(A)**, $p53^{-/-}RB^{-/-}$ BM-MSCs **(B),** $p53^{-/-}$ ASCs **(C)** and $p53^{-/-}RB^{-/-}$ ASCs **(D)**. Normal host bone (B), normal bone marrow (BM), tumoral bone marrow (TBM), reactive bone (RB) and tumoral osteogenic areas (Os) are indicated. Blue arrows indicate the presence of osteogenic tumoral cells in the BM niche and yellow arrows indicate mitotic cells.

Figure S2: Representative H&E staining of a human OS primary sample arisen in distal femur and obtained from the Hospital Universitario Niño Jesús (Madrid, Spain) upon signed informed consent and approval from the local ethics committee. Healthy bone (B) and tumoral osteogenic areas (Os) are indicated.

Figure S3: Formation of mineralized osteoblastic metastasis in lung. GFP immuno-staining (top panels) and the corresponding isotype controls (bottom panels) of metastatic nodules in the lungs of mice intra-bone inoculated with $p53^{-/-}RB^{-/-}$ BM-MSCs. The metastatic process includes the extravasation of GFP+ tumoral cells from blood vessels (Vs; left panels), the migration, homing and proliferation of metastatic GFP+ cells (middle panels) and the mineralization of metastatic lesions with osteogenic potential (right panels).

Figure S4: µ-CT imaging of OS generated by $p53^{-/-}$ and $p53^{-/-}RB^{-/-}$ ASCs. µ-CT images of bone surface (isosurface) **(A)**, maximum intensity projection **(B)** and representative longitudinal and sagital orthogonal sections **(C)** of a control leg, and legs periosteally-inoculated with $p53^{-/-}$ ASCs and $p53^{-/-}RB^{-/-}$ ASCs. Compared to the control leg, changes in cortical bone intensity (black arrows), peri-bone formation (white arrows) and intra-marrow bone formation (grey arrows) resemble human OS features in legs inoculated with transformed ASCs.

Figure S5: Immunophenotypic profile of the parental MSCs (before Cre-mediated deletion of p53 and RB genes) analyzed by flow cytometry. Representative dot plots are shown for Sca-1, CD29, CD44, CD14, CD11b, and CD45. black lines represent the irrelevant isotypes. Red lines display antibody-specific staining.

Figure S6: Saos-2 conditioned medium enhances ALP activity in $p53^{-/-}RB^{-/-}$ BM-MSCs/ASCs. ALP activity per µg of protein in $p53^{-/-}RB^{-/-}$ BM-MSCs **(A)** and $p53^{-/-}RB^{-/-}$ ASCs **(B)** lysates after a 7-day treatment with Saos-2 conditioned media.

Figure S7: Proliferation in tumors generated by transformed MSCs in a ceramic bone-like environment model. Ki67 immuno-staining (left panels) and the corresponding isotype controls (right panels) evidencing proliferation in tumors after s.c. inoculation of $p53^{-/-}RB^{-/-}$ BM-MSCs with or without BMP-2 and embedded or not in HA/TCP ceramic implants. Ceramic pieces (Cer) and tumoral osteogenic areas (Os) are indicated.

Table 1. In vivo tumor formation ability of wt, $Rb^{-/-}$, $p53^{-/-}$, $Rb^{-/-}p53^{-/-}$ BM-MSCs/ASCs.

MSC type	Subcutaneous inoculation§			Intra-bone inoculation			Periosteal inoculation		
	Tumor incidence	Latency	Histological analysis	Tumor incidence	Latency	Histological analysis	Tumor incidence	Latency	Histological analysis
BM-MSCs									
Wt	0/8	-	-	0/5	-	-	-	-	-
$Rb^{-/-}$	0/9	-	-	0/6	-	-	-	-	-
$p53^{-/-}$	6/12	65-148 (107)*	Leiomyosarcoma	4/9	94-116 (105)*	Osteosarcoma	2/2	(110)	Osteosarcoma
$Rb^{-/-}$ $p53^{-/-}$	19/25	31-109 (65)*	Leiomyosarcoma	10/14	48-156 (93)*	Osteosarcoma	4/4	24-20 (22)*	Osteosarcoma
ASCs									
Wt	0/8	-	-	0/5	-	-	-	-	-
$Rb^{-/-}$	0/8	-	-	0/5	-	-	-	-	-
$p53^{-/-}$	4/8	43-123 (74)	Leiomyosarcoma	5/9	126-173 (157)	Osteosarcoma	1/4	(120)	Osteosarcoma
$Rb^{-/-}$ $p53^{-/-}$	7/13	43-69 (54)	Leiomyosarcoma	7/9	100-174 (128)	Osteosarcoma	6/6	63-90 (77)*	Osteosarcoma

(§) Data from Rubio et al.,2010 (ASCs) & 2012 (BM-MSCs) [22, 23]. (*) Range of days for tumor development (mean).

Table 2. In vivo tumor formation ability of $Rb^{-/-}p53^{-/-}$ BM-MSCs/ASCs inoculated subcutaneously with BMP2 and using or not ceramic-fibrin based implants.

MSC type	Treatment	s.c. inoculation			ceramic implant		
		Tumor incidence	Latency	osteoid in tumors[§]	Tumor incidence	Latency	osteoid in tumors[§]
BM-MSC-$Rb^{-/-}p53^{-/-}$	Control	3/3	47*	-	5/5	24*	+ (next to ceramic)
	BMP2	3/3	47*	++ (throughout tumor)	5/5	24*	+++ (throughout tumor)
ASC-$Rb^{-/-}p53^{-/-}$	Control	3/4	57*	-	8/8	53*	+ (next to ceramic)
	BMP2	3/3	39*	++ (throughout tumor)	7/7	55*	+++ (throughout tumor)

(*) Range of days for tumor development (mean). ([§]) Approximate extension and distribution pattern of osteoid areas in osteosarcomas based on histological analysis and referred to the total area of the tumor: -: no osteoid observed; +: less than 5%; ++: 5-15%; +++: more than 15%

Rubio et al. Figure 1

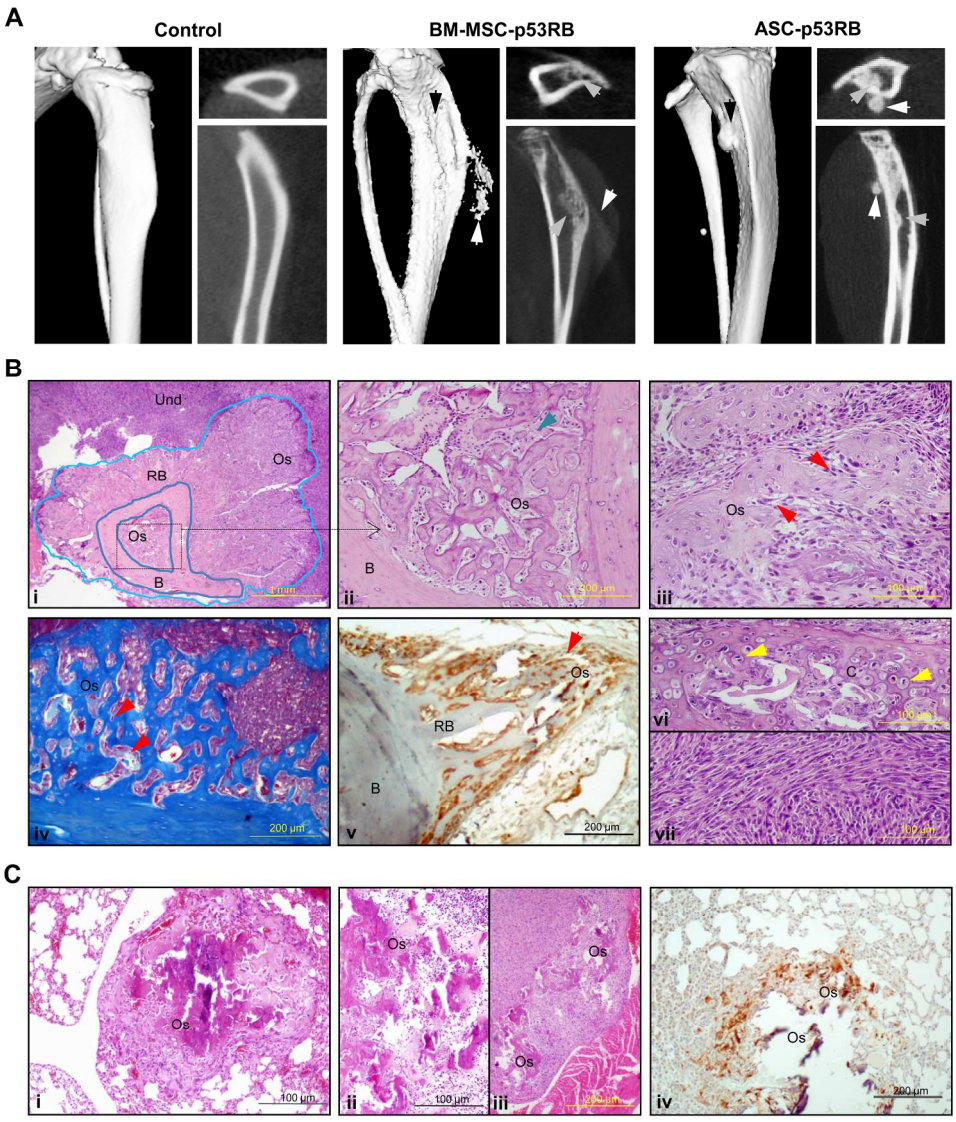

Development of OS upon intra-bone inoculation of p53-/- and p53-/-RB-/- BM-MSCs/ASCs
199x246mm (300 x 300 DPI)

Rubio et al. Figure 2

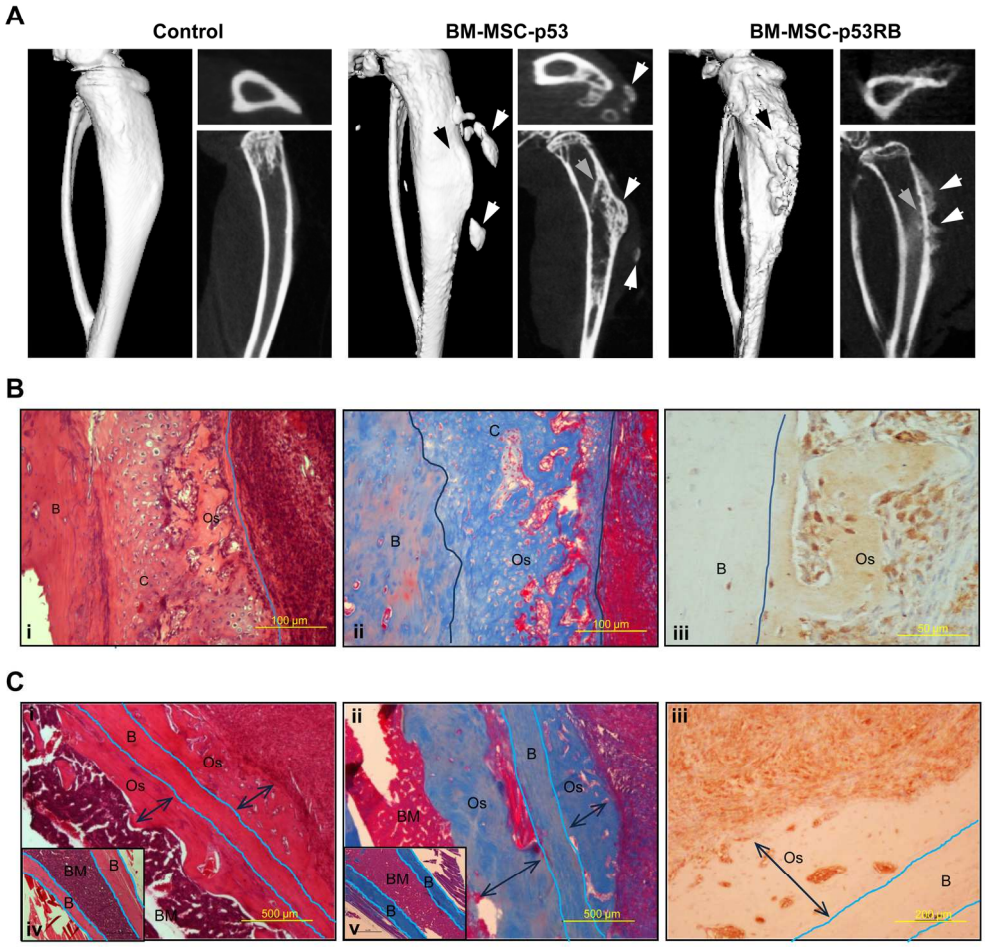

Development of OS upon periosteal inoculation of p53-/- and p53-/-RB-/- BM-MSCs/ASCs
170x181mm (300 x 300 DPI)

Rubio et al. Figure 3

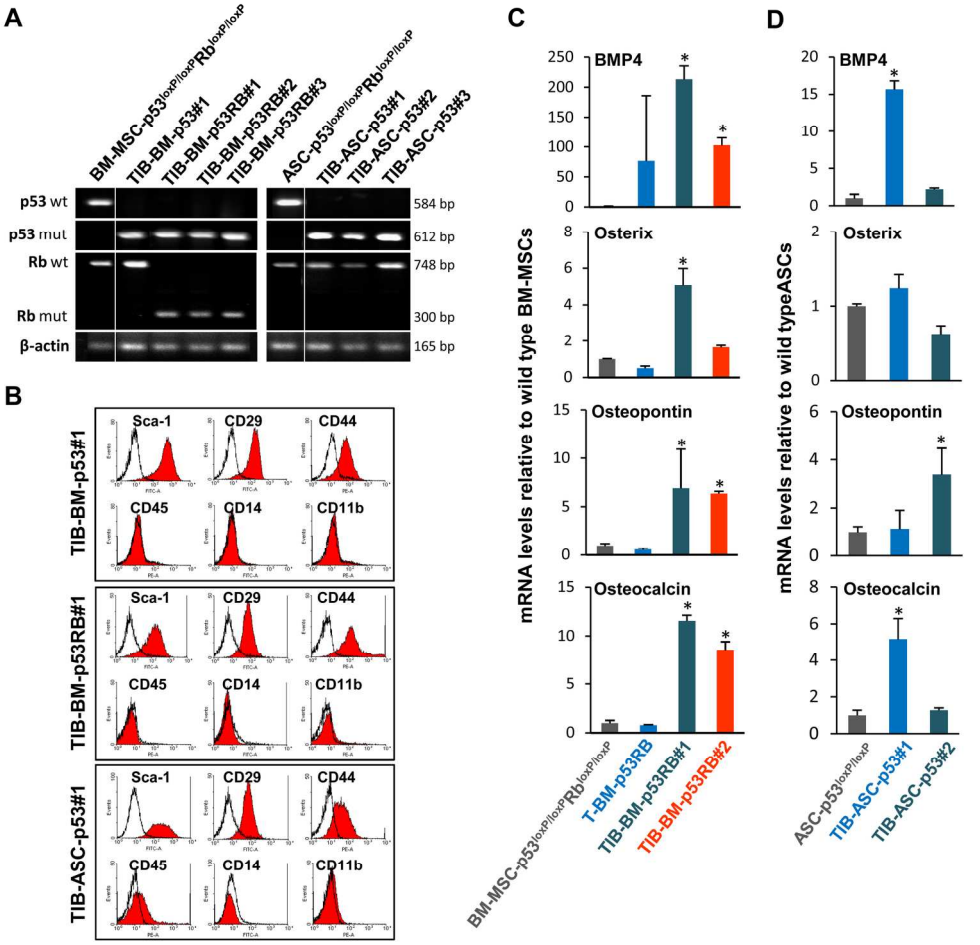

Immortalized cell lines ex vivo derived from primary OS generated by tumorogenic p53- and p53/RB-deficient BM-MSCs/ASCs show a MSC phenotype and express osteogenic markers
173x182mm (300 x 300 DPI)

Rubio et al. Figure 4

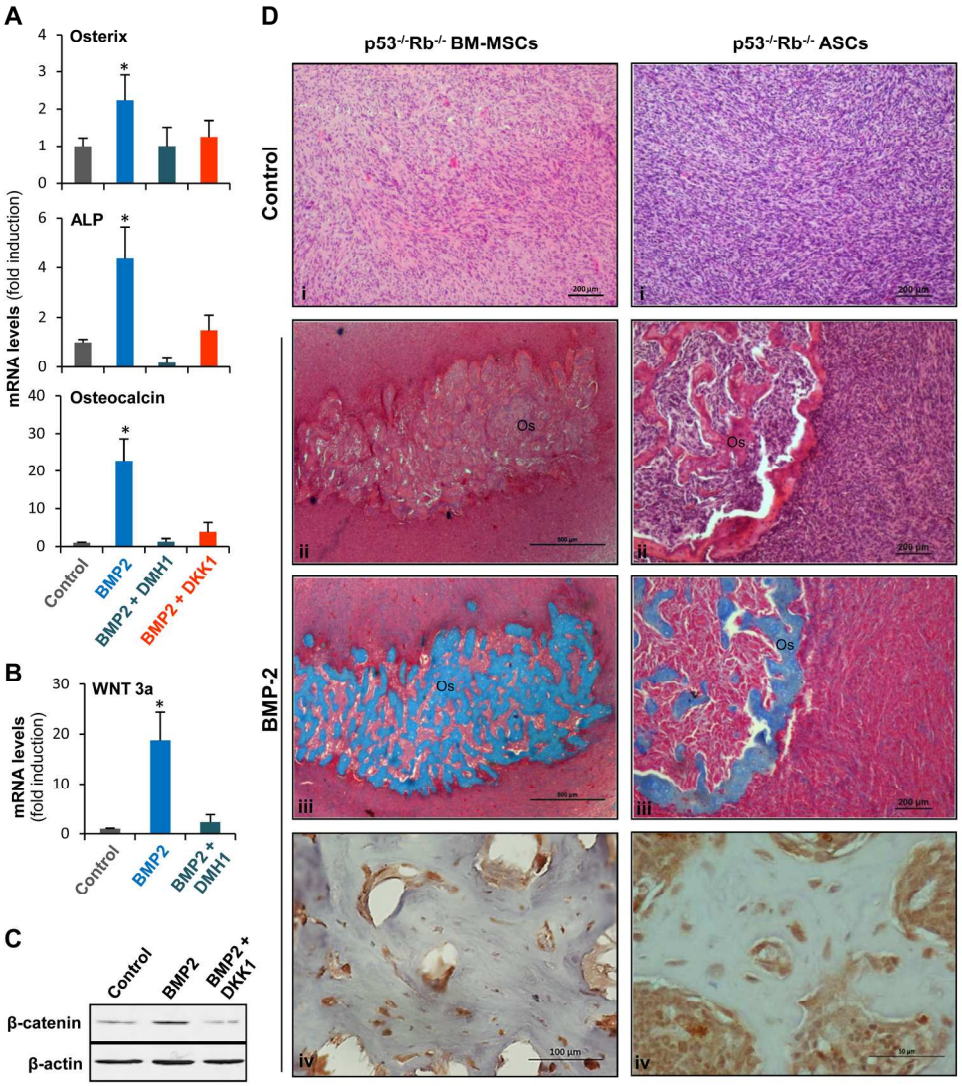

BMP-2 administration promotes osteogenic differentiation through the activation of Wnt singnaling and OS development upon subcutaneous inoculation
197x231mm (300 x 300 DPI)

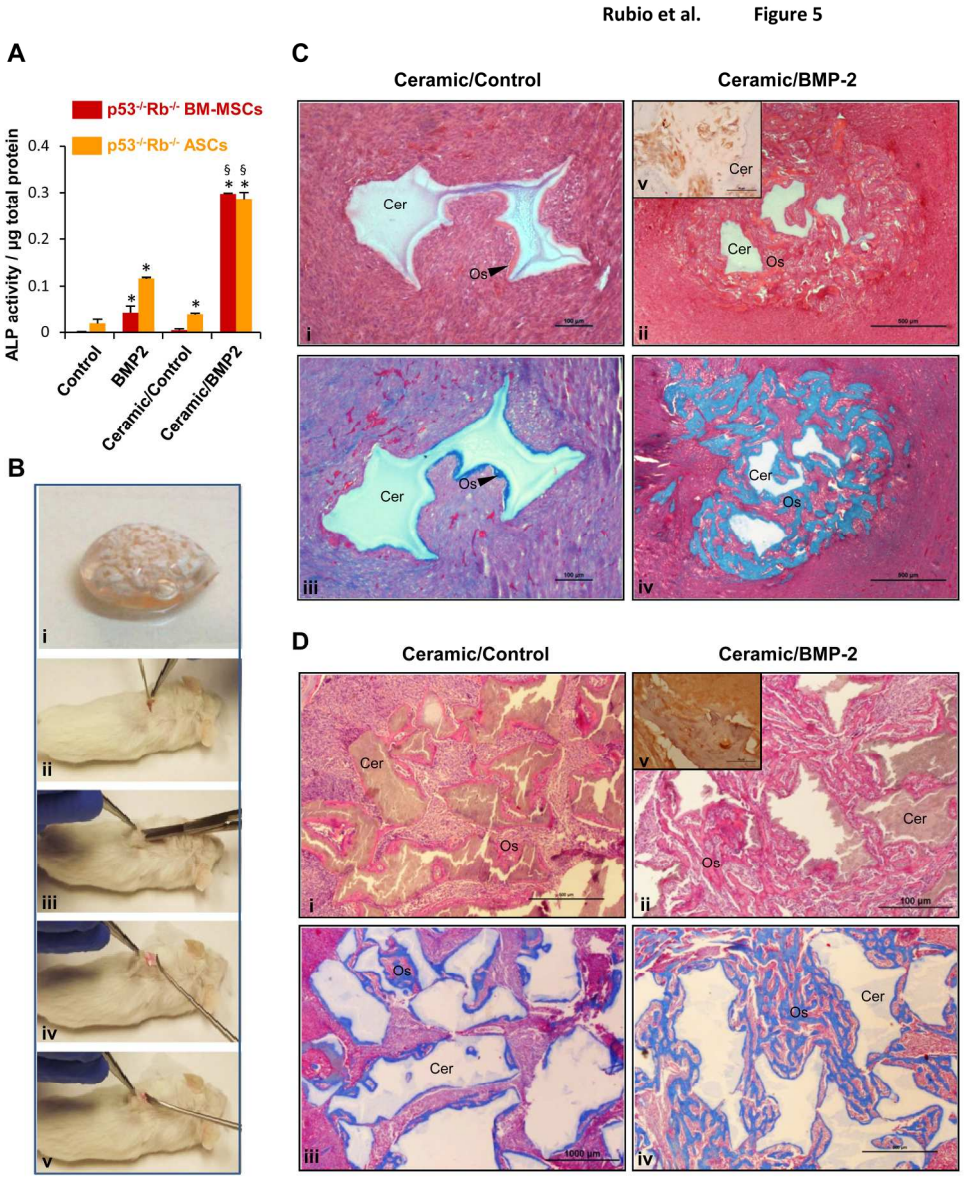

A ceramic bone-like environment model allows testing of individual bone factors involved in OS development
201x246mm (300 x 300 DPI)

Table S1: Sequences of primers used in the present study.

Gene	Oligo	Sequence (5´-3´)
Rb	Fw	GGCGTGTGCCATCAATG
	Rev	AACTCAAGGGAGACCTG
p53	Fw Wt	AAGGGGTATGAGGGACAAGG
	Fw mut	CACAAAAACAGGTTAAACCCAG
	Rev	GAAGACAGAAAAGGGGAGGG
BMP-4	Fw	TAAGAACTGCCGTCGCCATT
	Rev	GGCCACAATCCAATCATTCC
ALP	Fw	CCAGCA GT TCTCTCTTGG
	Rev	CTGGGAGTCTCATCCTGAGC
Oxterix	Fw	GCAAGGCTTCGCATCTGAAAA
	Rev	AACTTCTTCTCCCGGGTGTGA
Osteocalcin	Fw	CTGACCCTGGCTGCGCTCTG
	Rev	GGCTGGGGACTGAGGCTCCA
Osteopontin	Fw	TGCTTTTGCCTGTTTGGCAT
	Rev	TTCTGTGGCGCAAGGAGATT
WNT3A	Fw	ATGTGAGCTCGCATGGCATAG
	Rev	GACGTAGCAGCACCAATGGAA
β-actin	Fw	GCCATCCAGGCTGTGCTGTC
	Rev	TGAGGTAGTCTGTCAGGTCC

Table S2. Grading of osteosarcomas derived from intra-bone implanted transformed MSC according to the French Federation of Comprehensive Cancer Centers (FNCLCC) system.

MSC type	Tumor	FNCLCC scoring*				
		tumor differentiation areas		necrosis	mitosis	total score (tumor grade)**
		osteoid/ chondroid	distant to bone			
BM-MSC-p53$^{-/-}$	#1	1	3	1	2	**6 (III)**
	#2	1	3	0	3	**6 (III)**
	#3	1	3	1	3	**7 (III)**
BM-MSC-p53$^{-/-}$Rb$^{-/-}$	#1	1	3	1	3	**7 (III)**
	#2	1	3	0	3	**6 (III)**
	#3	1	3	0	2	**5 (II)**
ASC-p53$^{-/-}$	#1	1	3	0	1	**4 (II)**
	#2	1	3	1	1	**5 (II)**
	#3	1	3	0	1	**4 (II)**
ASC-p53$^{-/-}$Rb$^{-/-}$	#1	1	3	0	1	**4 (II)**
	#2	1	3	1	1	**5 (II)**
	#3	1	3	0	3	**6 (III)**

(*) This three grade system is based on the accumulative scoring obtained by three factors: i) tumor differentiation [1 (more differentiated) to 3 (less differentiated)]; ii) presence of necrosis [(0 (no necrosis); 1 (<50% of necrosis); or 2 (>50% of necrosis)]; and iii) mitosis count [1 (0-9 mitotic counts in a high power field (HPF; 40x); 2 (10-19 mitotic counts in a HPF); or 3 (>20 mitotic counts in a HPF)]. Grades I, II and III correspond to accumulative scores of 2-3, 4-5 and 6-8 respectively [38].

(**) According to the FNCLCC system, the total score of the tumor is calculated using the tumor differentiation score corresponding to the less differentiated area of the tumor (distant to the bone area).

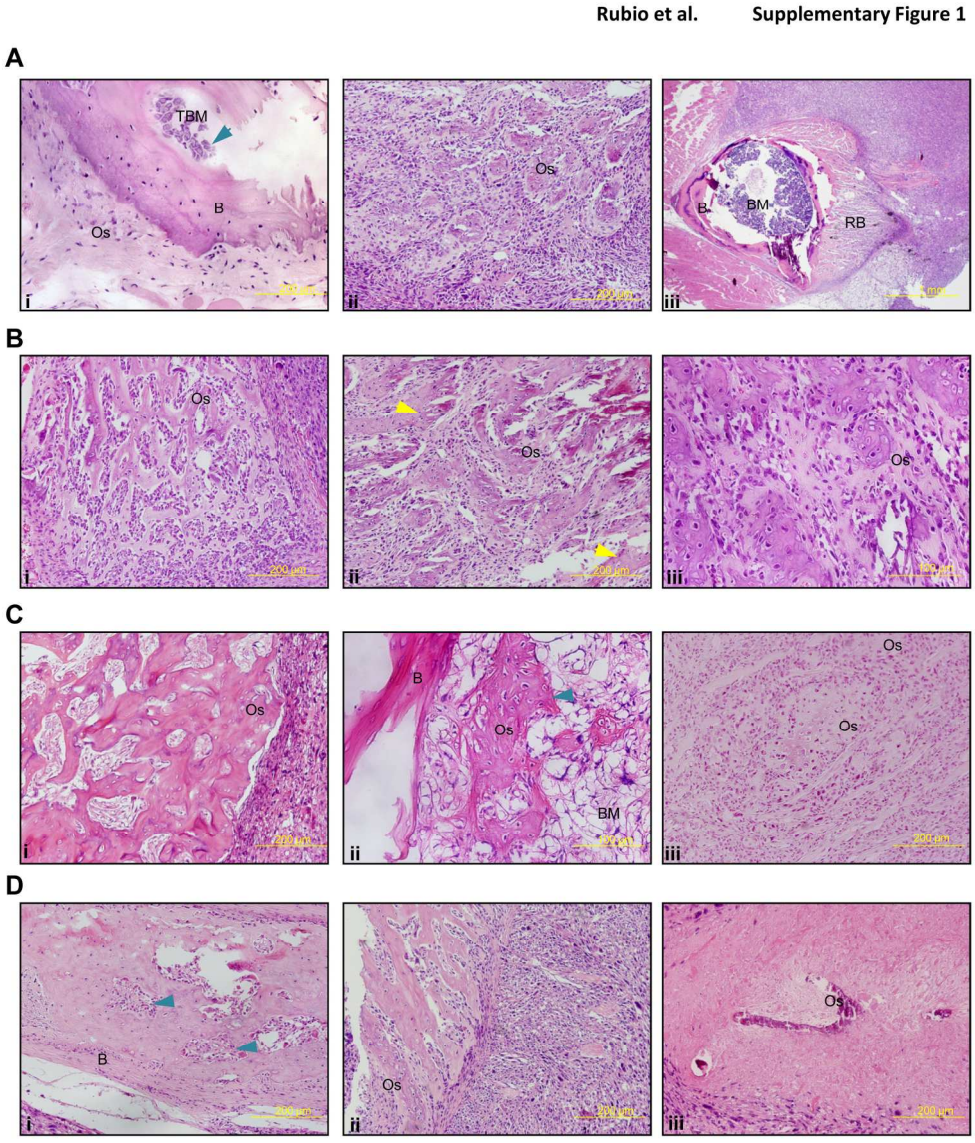

Development of OS upon intra-bone inoculation of p53-/- and RB-/-p53-/- BM-MSCs/ASCs
188x217mm (300 x 300 DPI)

Rubio et al. Supplementary Figure 2

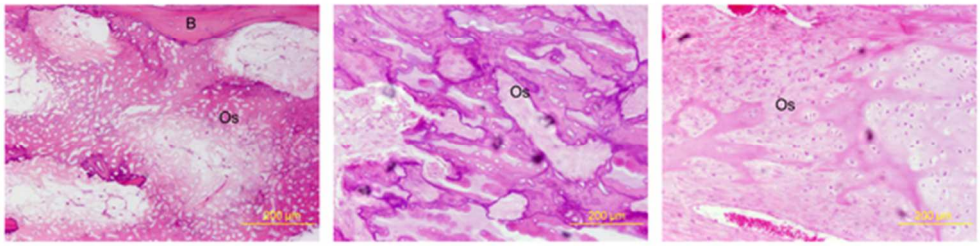

Representative H&E staining of a human OS primary sample
50x16mm (300 x 300 DPI)

Rubio et al. Supplementary Figure 3

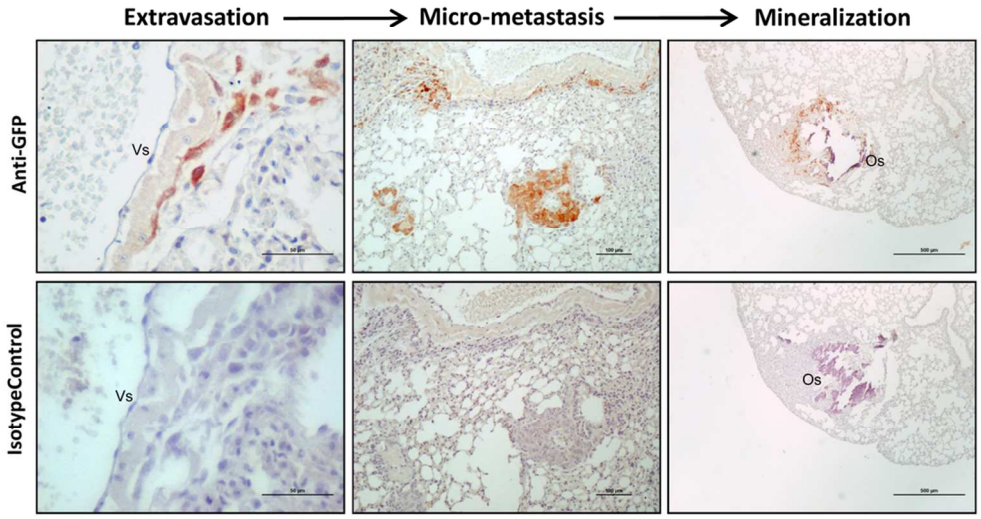

Formation of mineralized osteoblastic metastasis in lung
98x58mm (300 x 300 DPI)

Rubio et al. Supplementary Figure 4

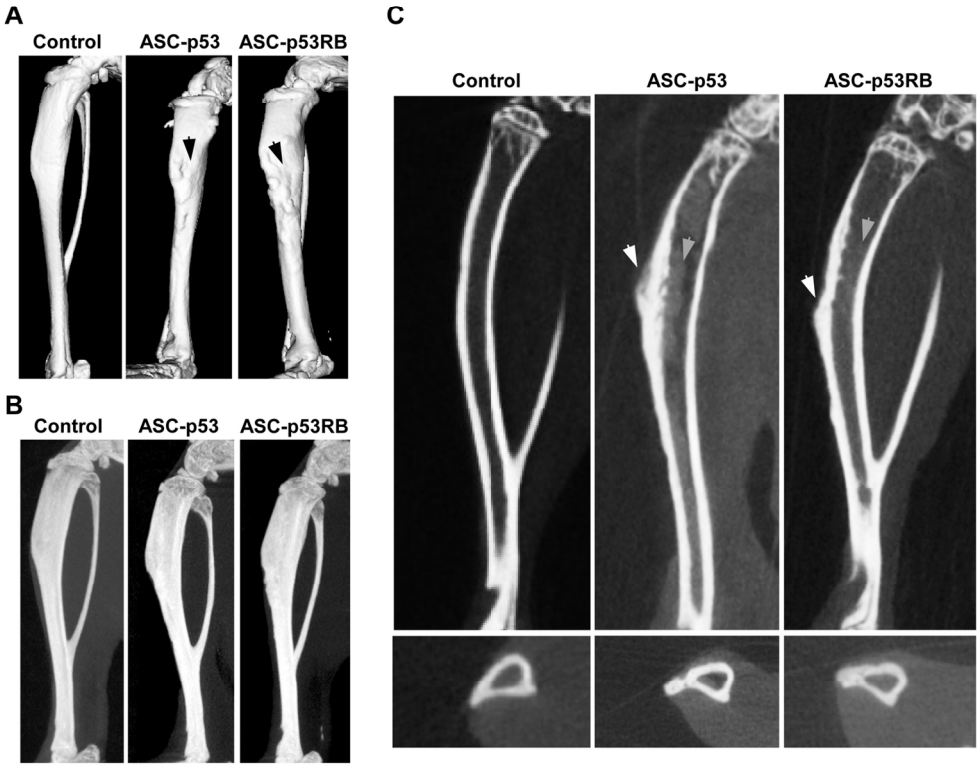

µ-CT imaging of OS generated by p53-/- and p53-/-RB-/- ASCs
142x123mm (300 x 300 DPI)

Rubio et al. Supplementary Figure 5

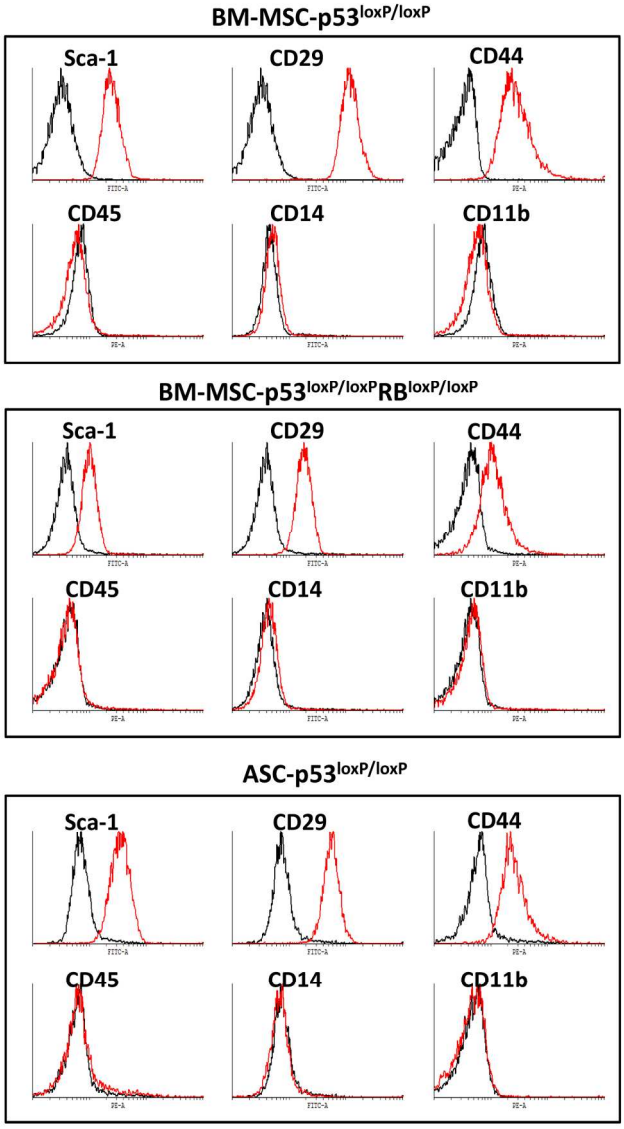

Immunophenotypic profile of the parental MSCs
187x344mm (300 x 300 DPI)

Rubio et al. Supplementary Figure 6

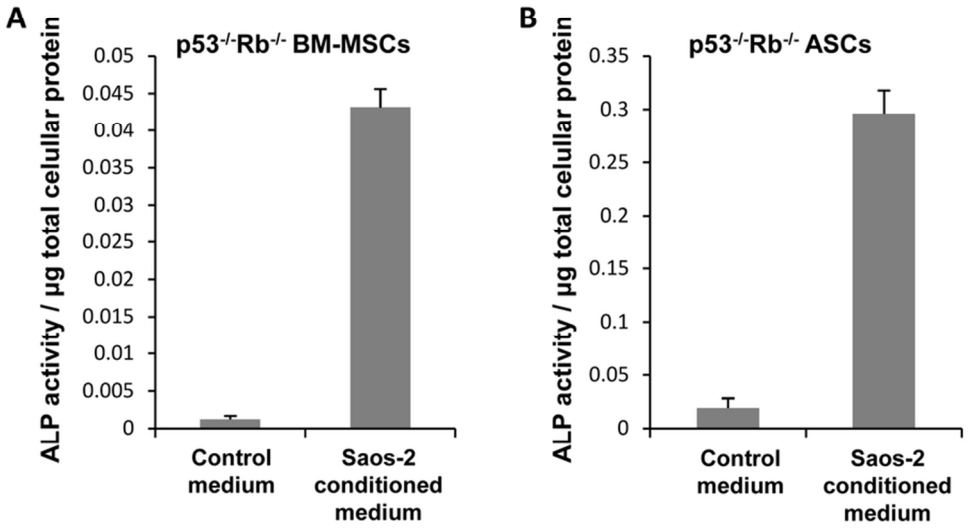

Saos-2 conditioned medium enhances ALP activity in p53-/-RB-/- BM-MSCs/ASCs
79x50mm (300 x 300 DPI)

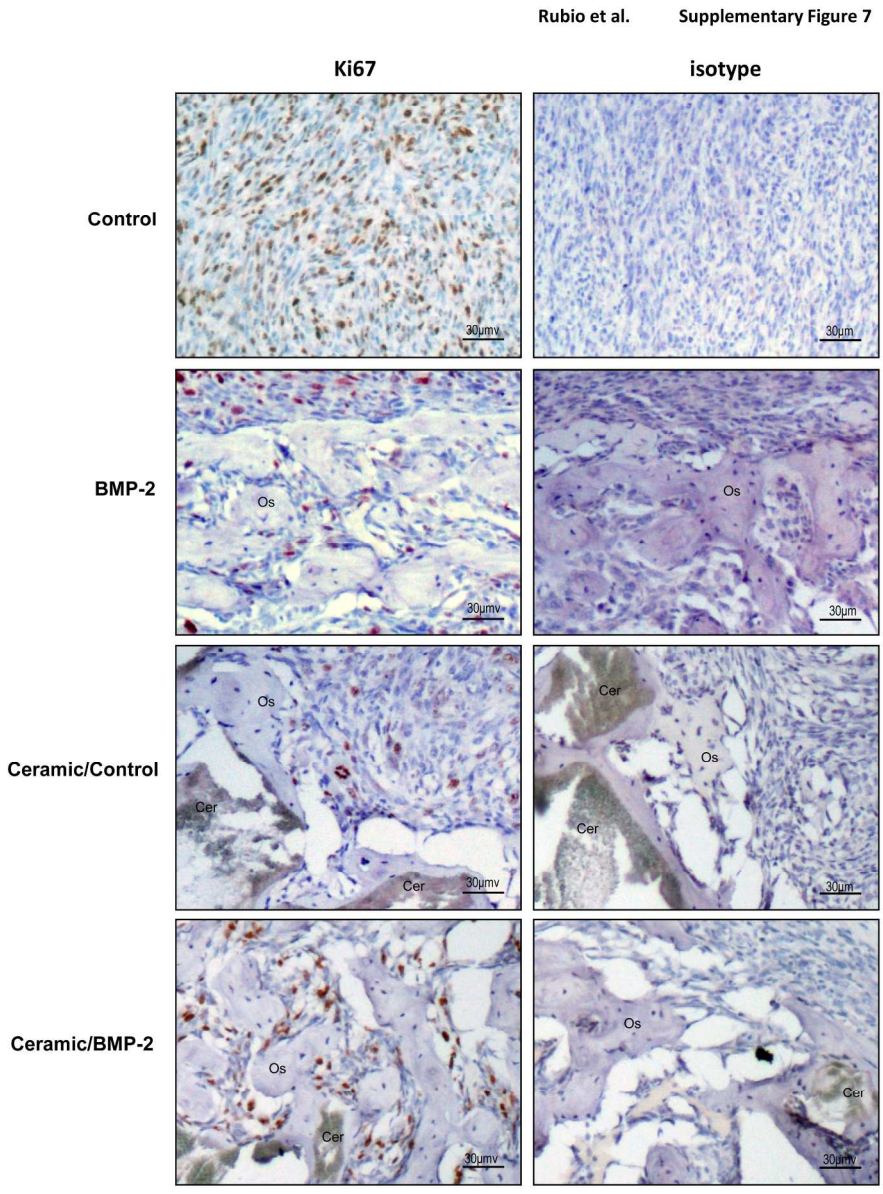

Proliferation in tumors generated by transformed MSCs in a ceramic bone-like environment model
216x289mm (300 x 300 DPI)